Microscopic Reaction Mechanism of Formic Acid Generated During Pyrolysis of Cellulosic Insulating Paper

Hanbo Zheng (hanbozheng@163.com)
Guangxi University https://orcid.org/0000-0002-7660-7293
Enchen Yang
Guangxi University
Xufan Li
Guangxi University
Tao Yang
State Grid Henan Electric Power Research Institute
Zijian Wang
Guangxi University
Yongji Feng
Guangxi University

Research Article

Keywords: Cellulosic insulation, Formic acid, ReaxFF, Silanization derivatization

Posted Date: February 15th, 2021

DOI: https://doi.org/10.21203/rs.3.rs-223461/v1

Microscopic reaction mechanism of formic acid generated during pyrolysis of cellulosic insulating paper

Hanbo Zheng · Enchen Yang · Xufan Li · Tao Yang · Zijian Wang · Yongji Feng

Abstract: Cellulosic insulating paper is the component part of the insulation in power transformers. Under thermal stress inside the transformer, cellulosic insulating paper degrades to generate formic acid that will dissolve in insulating oil. In addition, the generation of formic acid further accelerates the aging process of insulating paper. This study took cellulose molecule with DP of 2 that was composed of D-glucose as the research object, the ReaxFF reaction force field was used to simulate the high temperature thermal aging process of cellulose. This study obtained the main reaction pathways of cellulose pyrolysis to generate formic acid. During the pyrolysis process, the number of formic acid molecules presented short-term fluctuations, which was the phenomenon of disappearance and regeneration of formic acid molecules. The combined element tracing method obtained three pathways of cellulose pyrolysis to generate formic acid: 1) The ether group oxygen atom O_5(O'_5) and C_1(C'_1) form a carbonyl group to generate formic acid. 2) Dehydrogenation of the primary alcohol hydroxyl group and the attached C atom form a carbonyl group to generate formic acid. 3) Dehydrogenation of the secondary alcohol hydroxyl group and the attached C atom form a carbonyl group to generate formic acid. Statistics found that the generation of formic acid molecules mainly come from the first pathway. The pre-exponential factor and activation energy of the calculated pyrolysis model were consistent with the experimental results. This study designed the accelerated thermal aging experiment of oil-paper insulation. The silanization derivatization method was used to detect the formic acid generated by the aging of insulating paper, which further verified the feasibility of formic acid as an index for evaluating the aging of cellulosic insulating paper.

Keywords Cellulosic insulation · Formic acid · ReaxFF · Silanization derivatization

---

Hanbo Zheng (✉) · Enchen Yang · Xufan Li · Zijian Wang · Yongji Feng
School of Electrical Engineering, Guangxi University,
Nanning 530004, Guangxi, China
e-mail: hanbozheng@163.com

Tao Yang
State Grid Henan Electric Power Research Institute,
Zhengzhou 450002, Henan, China.

Introduction

Oil-immersed power transformer is the key equipment for power transmission and transformation, its life depends mainly on the performance of oil-paper insulation. The oil-paper insulation system is affected by the synergistic effect of heat, electric field, chemical corrosion and other factors, resulting in the performance degradation. When local overheating occurs inside the transformer, the temperature is as high as 1000°C (Standard 2006; Wang et al. 2012), and long-term local overheating causes thermal aging of the insulating paper. Lundgaard et al (2004, 2008) studies have shown that formic acid will be generated after aging of insulating paper. Compared with the CO, CO_2 and alcohols produced by thermal aging of cellulosic insulating paper (Gao et al. 2012; Zheng et al. 2020), the presence of formic acid will accelerate the aging process of insulating paper. Formic acid is a medium strong acid with strong ionization capacity, the ionized H^+ only acts as a catalyst and is not consumed in the hydrolysis and degradation reaction of insulating paper, so the H^+ content of insulating paper will increase with aging to form a self-accelerating mechanism (Lelekakis et al. 2014). In the aging process of insulating paper, the small volume of formic acid molecules can fully dissolve in the insulating paper to destroy the crystalline and amorphous regions of the insulating paper, which significantly accelerates the aging rate of the insulating paper (Ingebrigtsen et al. 2004; Lundgaard et al. 2005; Gao S et al. 2020). The influence of carboxylic acid on the life of insulating paper is related to its dielectric constant, the dielectric constant of formic acid is much higher than other carboxylic acids generated by the aging of oil-paper insulation (Mo et al. 2016). Kouassi et al (2018) tested the aging rate of insulating paper under the action of three low molecular weight carboxylic acids, and found that the aging rate of insulating paper was the fastest under the action of formic acid. Vahidi et al (2017) studied the influence of different carboxylic acids on the conductivity of insulating oil, of which formic acid had the greatest influence on the conductivity of insulating oil. At the same time, formic acid will increase the probability of partial discharge of the insulating oil paper and the corrosion of metal parts such as iron core windings (Wada et al. 2014). Furfural (2-FAL) is a commonly used marker for evaluating the aging status of transformers (Urquiza et al. 2015), but Tang et al (2017) found that the content of furfural in transformer oil showed a downward trend in the later

stages of aging, which was completely inconsistent with the continuous aging of insulating paper. The oxidation of alcohols and aldehydes will generate carboxylic acids, so the stability of carboxylic acids is higher than that of alcohols and aldehydes. Azis et al (2014) studied scrapped transformers and found that there was an exponential relationship between the tensile strength of insulating paper and the content of low molecular weight carboxylic acids, thus proposed that low molecular weight carboxylic acids in insulating oil could be used as a potential indicator of the aging of insulating paper. Therefore, as a kind of low molecular weight carboxylic acid produced by the aging of insulating paper, formic acid is a potential indicator for evaluating the aging state of insulating paper.

Early research on pyrolysis of cellulosic insulating paper mostly used experimental methods. The pyrolysis process of polymer compounds involves complex chemical changes, and the micro-mechanism of cellulosic insulating paper at high temperature is difficult to obtain from traditional experiments. With the development of quantum mechanics theory system and computer technology, molecular simulation has been widely used in many fields (English et al. 2015; Tang et al. 2015). In the increasingly complex field of high-voltage insulation, molecular simulation technology has been used to analyze the aging mechanism of insulating materials with remarkable success (Li et al. 2019; Du et al. 2020). ReaxFF (Adri et al. 2001) is a reactive molecular dynamics force field that can describe the formation and breaking of chemical bonds, it is widely used to describe complex chemical reaction processes. The ReaxFF force field method can clearly describe the structural changes of reactants and reveal their reaction mechanisms. Shi et al (2001) used ReaxFF force field to study the generation principle and destruction mechanism of water molecules during the high temperature pyrolysis of insulating paper, it analyzed the generation path and generation law of water molecules at different temperatures. The initial reaction mechanism of cellulose pyrolysis was studied by the ReaxFF force field, it obtained the detailed reaction pathway of cellulose pyrolysis to produce glycolaldehyde, hydroxyacetone and 2-hydroxypropionaldehyde (Zheng et al. 2016). Paajanen et al (2017) used ReaxFF force field to study the initial stage of the thermal decomposition process of cellulose molecules, the most commonly observed products are glycolaldehyde and formic acid. Zhang et al (2020) used the ReaxFF reaction kinetic model to study the microscopic mechanism of methanol generation during thermal aging and cracking

of insulating paper, which obtained the reaction path of the pyrolysis of insulating paper to methanol. The study showed that methanol could be used to evaluate the aging state of insulating paper at the initial stage of aging. These research results have laid a theoretical foundation for using the ReaxFF reaction dynamic field, which study the production mechanism of formic acid during the high-temperature pyrolysis of insulating paper.

To study the formation mechanism of formic acid during high temperature thermal aging of insulating paper, this paper built a cellulose molecular model. This study used the ReaxFF reaction force field to simulate the pyrolysis reaction of a multi-molecular system. It analyzed the generation pathway and law of formic acid from the atomic level. This study established the cellulose pyrolysis models at different temperatures, which analyzed the influence of temperature on the formation and pathway of formic acid. This paper designed oil-paper insulation accelerated thermal aging experiments, the silanization derivatization method was used to detect the formic acid generated by the aging of the insulation paper.

Molecular simulation section

ReaxFF force field calculation principle

The selection of force field is an important part in molecular dynamics simulation. As a new generation of force field, ReaxFF can truly reflect the formation, transition and fracture process of chemical bonds in the system. The ReaxFF reaction force field takes the bond level (BO) as the core, which calculates the BO from the distance between two atoms. BO judges the connectivity of atoms at the current moment, characterizes the breaking and formation of chemical bonds (Adri et al. 2001). Suppose the distance between two atoms at the current moment is r_{ij}, then the uncorrected bond level between the two atoms is shown in Eq. (1).

$$\begin{aligned} BO'_{ij} &= BO^{\sigma}_{ij} + BO^{\pi}_{ij} + BO^{\pi\pi}_{ij} \\ &= \exp[p_{bo1} \times (\frac{r_{ij}}{r_0^{\sigma}})^{p_{bo2}}] + \exp[p_{bo3} \times (\frac{r_{ij}}{r_0^{\pi}})^{p_{bo4}}] + \exp[p_{bo5} \times (\frac{r_{ij}}{r_0^{\pi\pi}})^{p_{bo6}}] \end{aligned} \quad (1)$$

As in Eq. (1), BO'_{ij} denotes a single bond, BO^{π}_{ij} denotes a double bond, $BO^{\pi\pi}_{ij}$ denotes a triple bond, P_{bo} denotes a bond parameter, r_0^{σ}, r_0^{π}, $r_0^{\pi\pi}$ denotes atomic parameters. On this basis, the ReaxFF force field corrects the over-coordinated bond poles and obtains the corrected bond level BO_{ij}. BO_{ij}=0.3 is used as the

criterion of whether the product is generated. When $BO_{ij} \geqslant 0.3$, it is considered that the chemical bond is formed and the product generates, otherwise the chemical bond is broken.

ReaxFF defines the interaction energy between atoms as a function of the bond level. The system potential function E_{system} is the sum of the potential energy of each part of the molecule. The expression of the potential energy function is as follows:

$$E_{system} = E_{bond} + E_{lp} + E_{over} + E_{under} + E_{val} + E_{pen} + E_{triple} + E_{tors} + E_{conj} + E_{H-bond} + E_{vdWaals} + E_{Coulamb} \quad (2)$$

As in Eq. (2), E_{bond} denotes the bond energy, E_{lp} denotes the lone pair electron term, E_{over} and E_{under} denote the over-coordination energy correction terms, E_{val} denotes the valence energy term, E_{pen} denotes the penalty energy term, E_{triple} denotes the triple bond correction term, E_{tors} denotes the torsion energy item, E_{conj} denotes the conjugation item of the molecule, $E_{H\text{-}bond}$ denotes the hydrogen bonding item, $E_{vdWaals}$ denotes the non-bonded van der Waals force item, $E_{Coulomb}$ denotes the non-bonded Coulomb force item. According to the potential energy of the system at the current moment, the ReaxFF force field can calculate the distance between the atoms at the next moment. It calculates the bond level to get the atom connection at the current moment, which judges the composition of the chemical bond. The molecular dynamics simulation of chemical reaction process is realized by cyclic iteration.

ReaxFF- MD simulation details

The basic component of insulating paper for oil-immersed transformers is cellulose, it is formed by D-glucose through β-1,4-glycosidic linkage (Gao et al. 2019). The degree of polymerization of cellulose molecules is the number of glucose monomers, the degree of polymerization of the newly-running transformer insulation paper is between 1000 and 1200 (Wang et al. 2019). Mazeau et al (2003) conducted simulation experiments with cellulose chains of different lengths. It found that the cellulose chain models of different lengths behave basically the same in molecular conformation and physical and chemical properties. This paper aims to study the generation mechanism of formic acid during the high-temperature pyrolysis of insulating paper, rather than simulating the process of aging of insulating paper DP. To save calculation time and improve calculation efficiency,

this paper only constructed DP-2 cellulose molecular model. At the same time, the D-glucose monomer molecule can be used as a model to show the formation process of formic acid more intuitively. Fig. 1a shows the structural formula of cellulose molecular formed by connecting two D-glucose monomers. To facilitate subsequent analysis, the major atoms in the model are labeled by element categories. Fig. 1b shows molecular structure model of DP-2 cellulose molecule, the red atoms are O atoms, the gray atoms are C atoms, and the white atoms are H atoms. The two pyran rings in the cellulose molecule are connected by β-1,4-glycosidic bond. The C atom 1 on the pyran ring is connected to the ether group, the C atoms at positions 2, 3, and 4 are connected to a secondary alcohol hydroxyl group. The C atom at position 6 is connected to the primary alcohol hydroxyl group.

Molecular model construction

In this paper, AMS software is used to simulate the reaction molecular dynamics of cellulose thermal degradation mechanism with reasonable geometric conformation under given conditions (Zhang et al. 2020). Firstly, this study built an amorphous cell model containing 50 cellulose molecules with a density of 0.66g/cm^3. The initial size of the model is 35*35*35Å, geometric structure optimization and energy optimization were carried out for the constructed initial model. The density of the model was adjusted under the isothermal isobaric ensemble condition. The simulated temperature was set at 0K, the time was set at 5ps and the pressure was set at 500 MPa. Finally, the model density was adjusted to reach the actual cellulose density of 1.599/cm^3 (Tang et al. 2019), the optimized model size is 26.4*25.3*26.6Å. Then the model used the NVT canonical ensemble to set a simulated temperature of 100K and a time of 20ps, the model was treated with energy minimization that made the system in a stable state. Fig. 1d shows the optimized model.

The object of study in this paper is cellulose that only contains three elements of C, H and O, so CHO. ff field in ReaxFF field is selected (Chenoweth et al. 2008). Rensen et al (2000) proposed that the reaction kinetics method of temperature acceleration, which uses the transition state theory to accelerate the molecular transition by increasing the temperature, but it only allows the event of initial temperature to occur. Shi et al (2016) used the ReaxFF force field to study the generation of cellulose pyrolysis water molecules. It found that temperature

changes only affect the pyrolysis rate and the number of products, but the product generation path didn't change. High temperature can enhance the collision effect between molecules and ensure the whole simulation time within a reasonable range. Under the premise of keeping the model reasonable and improving the calculation efficiency, several times of pyrolysis simulation was conducted by setting the 0K-3000K temperature rise process in order to optimize the temperature setting. Finally, the model pyrolysis temperatures were set between 1600K-2600K, the pyrolysis time was set to 100ps and each step is 0.2fs. The pyrolysis process was completed under the NVT canonical ensemble. In addition to the temperature, the pyrolysis parameters of each system should be the same to ensure the reliability of the simulation results. To analyze the cracked products, the current reaction state of the system is recorded every 10 fs.

In the reaction process, electrostatic attraction makes the process of molecular interaction closely related to the electrostatic potential on the molecular surface. In this paper, the distribution of electrostatic potential (Lu et al. 2012) on the molecular van der Waals surface was analyzed to predict intermolecular reaction sites and intermolecular interactions. Fig. 1c shows the surface electrostatic potential distribution of cellulose molecule. In Fig. 1c, the darker blue area indicates the negative electrostatic potential, the darker red area indicates the positive electrostatic potential. The electrostatic potential value of the white area is near 0. Electrophilic reactions are prone to occur in areas with negative electrostatic potential. Nucleophilic reactions are prone to occur in areas with positive electrostatic potential. It can be seen from Fig.1c that the C-O bond site is in the blue region and is prone to nucleophilic reaction, while the red hydrogen atom site is prone to nucleophilic reaction. It can be seen that the C-O bond and H atom in the cellulose molecule show strong reactivity, so the C-O bond and H atom are the easiest to react during the pyrolysis of the cellulose molecule.

Experimental method and process

The reports on the research of carboxylic acid substances in oil-paper insulation are mostly to monitor the acid value of the insulation system during the aging process, and explore the influence of carboxylic acid substances on the degradation of oil-paper insulation (Cui et al. 2013; Ojha et al. 2017). There are few reports on

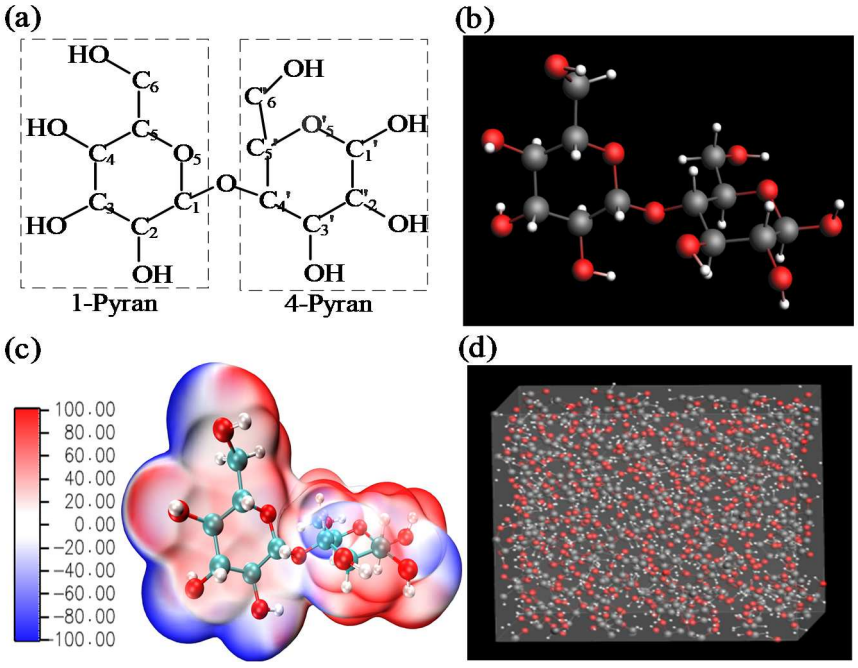

Fig. 1 **a** The main atoms of DP-2 cellulose molecule. **b** Molecular model of DP-2 cellulose molecule. **c** Electrostatic potential distribution on the surface of DP-2 cellulose molecule. **d** Amorphous unit cell optimized model.

the qualitative detection of the types of carboxylic acids produced during the aging process of oil-paper insulation. To verify the generation of formic acid from aging of insulating paper, this study designed the aging experiment of oil-paper insulation that conduct qualitative detection of formic acid. The experimental process is shown in Figure 2. Different from the detection of alcohols in transformer oil paper insulation (Zhang et al. 2021), the qualitative study of low molecular weight carboxylic acids is mostly done by derivatization and gas chromatography-mass spectrometry combined technology. The BSTFA silanization reagent has the advantages of high derivatization rate and simple detection process when detecting low molecular weight molecule carboxylic acid substances (Šťávová et al. 2012). Therefore, this study chose BSTFA silanization derivatization method to detect formic acid. Firstly, insulating oil and insulating paper with a mass ratio of 10:1 was dried in a drying oven for 48 hours. After drying, the insulating paper was put into insulating oil and insulation paper vacuumed immersion oil for 24 hours. Then the oil-paper insulation sample was placed in a 140°C aging box for accelerated thermal aging, the aging time was 5 days. The aging insulating paper was extracted by acetonitrile, then the extraction solution and BSTFA reagent with a volume ratio of 2:1 was placed a thermostat at 60°C for 60 minutes of silanization. Finally, the silanized samples were detected by a gas chromatography mass spectrometer.

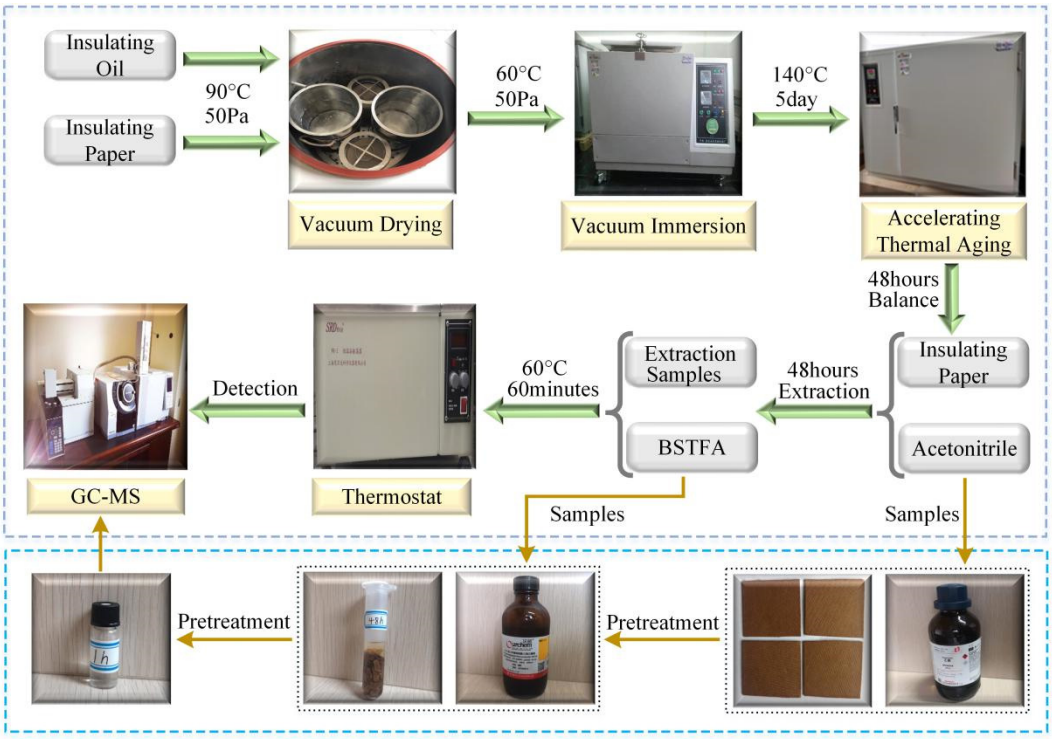

Fig.2 Oil-paper insulation thermal aging experiment and silanization detection for formic acid

Analysis of pyrolysis results

To study the evolution of formic acid with time during the pyrolysis of cellulose, the amounts of formic acid were counted at different simulated temperatures. Fig. 3 a-f shows the curve of the number of formic acid molecules changing with time under the pyrolysis conditions of 1600K-2600K. When the simulated temperature was different, the earliest time for formic acid molecules to appear in each system was different. The formic acid molecules started to appear after 40ps at 1600K, the number of formic acid molecules was less and the curve fluctuation was not obvious. When the simulated temperature was 1800K-2000K, formic acid molecules appeared around 10ps at the initial stage of pyrolysis. The amount of formic acid increased rapidly and presented a fluctuating upward trend. When the simulated temperature was 2200K-2600K, formic acid molecules appeared before 10ps. The amount of formic acid fluctuated to the peak and then dropped slightly at the end. As the pyrolysis temperature increased, the rate of increase in the number of formic acid molecules increased. When the temperature continued to rise, the peak number of formic acid molecules basically no longer changed. The increase of pyrolysis temperature advanced the peak time of the number of formic acid molecules. After the number of formic acid molecules reached the maximum, the number of formic acid molecules decreased slightly. There were still plenty of

formic acid molecules in the later stage of pyrolysis, indicating that formic acid molecules have better stability. During the pyrolysis process, the number of formic acid molecules would fluctuate. This phenomenon was due to the formation of a large number of small molecular fragments during the high temperature pyrolysis of cellulose molecules. The high-speed movement of molecules in the high temperature thermal field increased the frequency of intermolecular collisions, which resulted in secondary reactions between small molecules and formic acid. At the same time, formic acid may undergo an esterification reaction with the hydroxyl group on the cellulose molecule (Ese et al. 2014). Therefore, formic acid occasionally disappeared and regenerated. After analyzing the pathways, it was found that the generation pathways of formic acid molecules at different temperatures was the same. The temperature conditions of 1800K-2200K were taken as examples to analyze the formation process of formic acid molecules.

Generation pathways of formic acid molecules

The bond breaking process in chemical reactions is closely related to the bond energy of chemical bonds. The bond energy can be used to analyze the pyrolysis process of cellulose. Table 1 lists the bond energies involved in the main chemical bonds in the model (Zhang et al. 2020). The formation pathways of formic acid molecules were analyzed by observing the fracture and formation of molecular bonds of reactants in different pyrolysis states. According to the different types of bond energies in Table 1, it can be seen that the C-O bond in the cellulose molecule is most likely to be broken. The simulation results in this paper are consistent with this conclusion (Wang et al. 2017). For the convenience of analysis, the pyrolysis images are partially enlarged for broken bonds and bonding sites. The reacted molecular groups were marked, it marked the breakage and formation of chemical bonds with dashed lines.

The activity of O atoms at different positions of cellulose molecules varies greatly. The O_5 (O'_5) atom at the ether group and C_1 (C'_1) are more likely to form carbonyl, while O atoms at secondary alcohols (C_2, C_3 and C_4) and O atoms at primary alcohol C_6 are more difficult to dehydrogenate to form carbonyl. This paper analyzed the pyrolysis of cellulosic insulating paper at different temperatures.

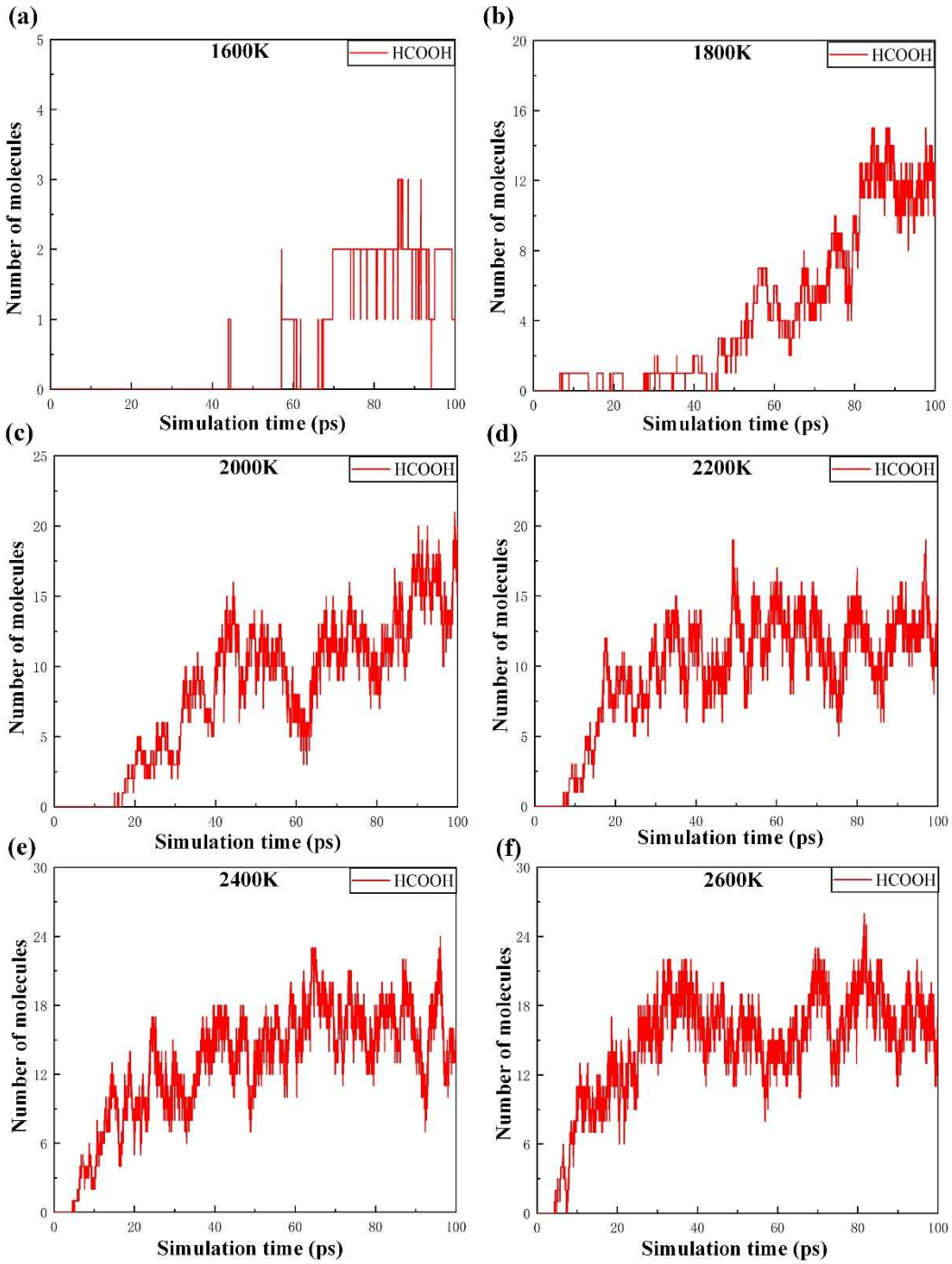

Fig. 3 Change curves of the number of formic acid molecules with pyrolysis time at 1600K-2600K

Table 1 Bond energy values of related chemical bonds

Bond type	Bond energy(kJ/mol)
C-O	326
C-C	332
C-H	414
O-H	464

The molecular generation pathways of formic acid can be divided into three categories. The three pathways of generating formic acid molecules are as follows:

1) The first pathway is that the ether group O_5 (O'_5) atom and the connected C_1 (C'_1) atom formed a carbonyl group to generate formic acid molecule. In the case of 1800 K, the formation process of the formic acid molecule was traced through the element tracer method. At 7.88ps, the O'_5 and C'_1 formed a carbonyl group after the ether group O'_5-C'_5 broke, as shown in Fig. 4a. At 8.09ps, the formic acid molecule was generated after the bond C'_1-C'_2 broke. At 29.26ps, the O_5 and C_1 formed a carbonyl group after the ether group O_5-C_5 broke, as shown in Fig. 4c. At 30.16ps, the bond C_1-C_2 broke, as shown in Fig. 4d. At 30.63ps, the bond O_6-C'_4 broke, as shown in Fig. 4e. At 35.1ps, the formic acid molecule was generated after the O atom grabbed H atom on the nearby group to form a hydroxyl group. Fig.5 shows the reaction formula of formic acid formation pathway 1. The key group carbonyl formed during the reaction that was marked with a dotted line. Statistics on the source of formic acid molecule generation under 1600K-2600K temperature conditions show that the generation of formic acid molecule mainly comes from this pathway. According to the analysis of molecular electrostatic potential and the comparison of molecular chemical bond energy, the bond C-O is most likely to break. Therefore, this pathway accounts for the highest proportion in the generation sources of formic acid molecules.

2) The second pathway is that formic acid molecule is generated after the primary alcohol hydroxyl group dehydrogenates to form carbonyl group. It is found that the pathway is to generate formaldehyde molecules firstly, then formic acid molecule is generated through a second reaction. In the case of 2000 K, the formation process of the formic acid molecule was traced through the element tracer method. Fig. 6a showed the structure of the primary alcohol hydroxyl group connected to C_6 at 0ps. At 29.75ps, the bond C_6-C_5 broke to form free radicals, as shown in Fig. 6b. At 30.42ps, formaldehyde molecule was generated after hydroxyl in the radical group dehydrogenated to form a carbonyl group, as shown in Fig. 6c. At 39.17ps, the C_6 atom in the center of the formaldehyde molecule occurred dehydrogenation reaction, as shown in Fig. 6d. At 54.28ps, the C_6 atom gained hydroxyl group, as shown in Fig. 6e. At 54.32ps, formic acid molecule was generated, as shown in Fig. 6f. Fig.7 shows the reaction formula of formic acid generation pathway 2. The key group carbonyl formed during the reaction that is marked with a dotted line. According to the oxidation reduction reaction, it can be known that formaldehyde is further oxidized to generate formic acid (Tojo et al. 2007). Statistics found that the number

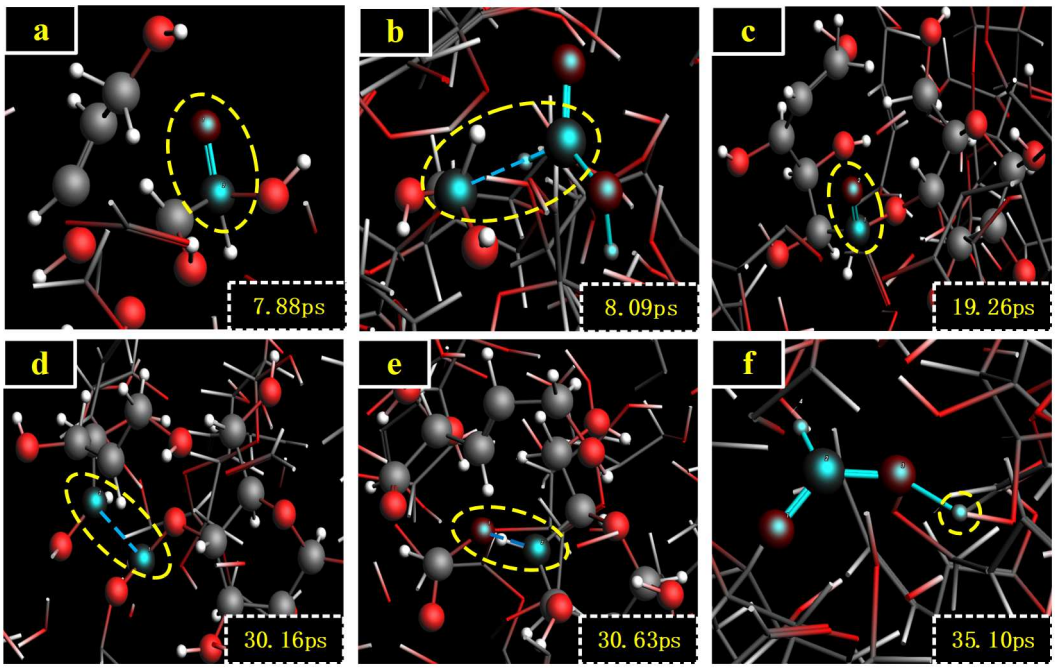

Fig. 4 Microscopic formation process of formic acid molecules. The picture reveals the generation pathway 1 of formic acid molecule during the pyrolysis of cellulose molecules

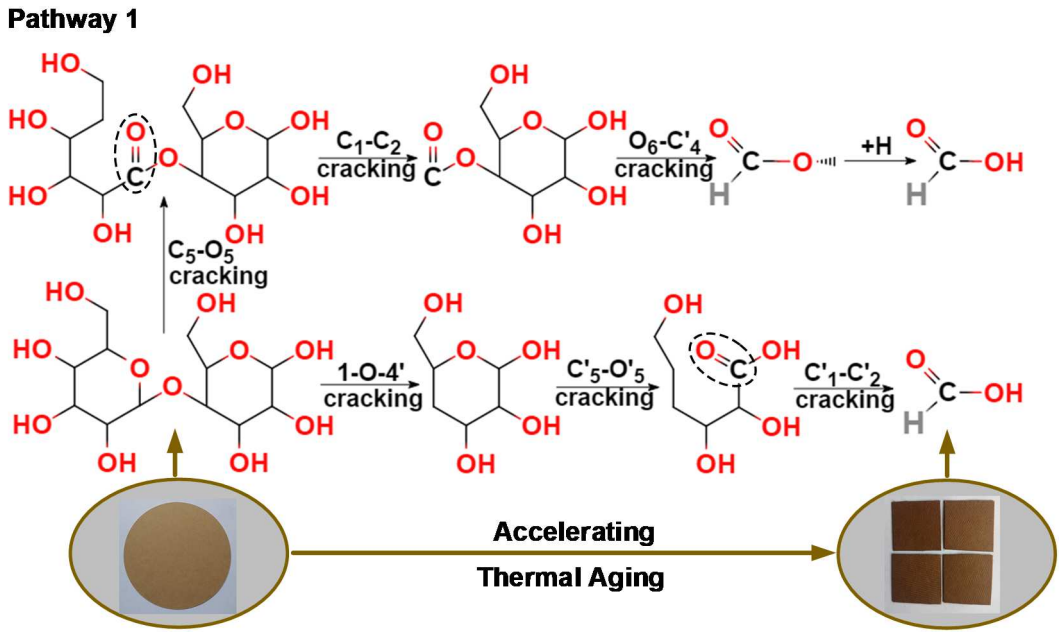

Fig. 5 Reaction formula of formic acid generation pathway 1. The pathway shows the breakage and formation of related chemical bonds

of formic acid molecules generated in this pathway was small. According to the analysis of molecular electrostatic potential and the comparison of molecular chemical bond energy, it can be known that this pathway required more energy to generate formic acid molecules than the first pathway.

3) The third pathway is that formic acid molecule is generated after the secondary alcohol hydroxyl group dehydrogenates to form carbonyl group. In the case of 2200 K, the generation process of the formic acid molecule was traced through the

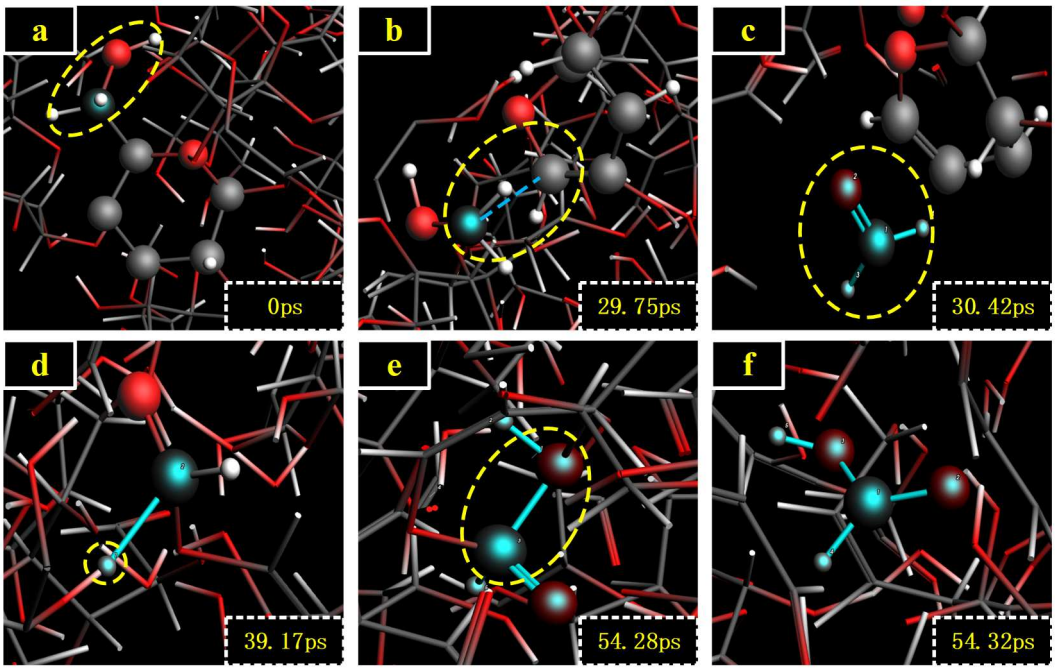

Fig 6 Microscopic formation process of formic acid molecules. The picture reveals the generation pathway 2 of formic acid molecule during the pyrolysis of cellulose molecules

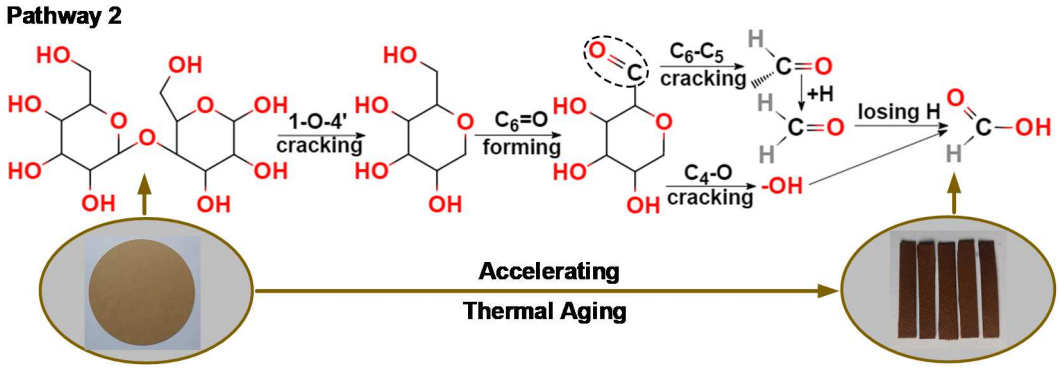

Fig.7 Reaction formula of formic acid generation pathway 2. The pathway shows the breakage and formation of related chemical bonds

element tracer method. The pathway to form formic acid molecules is shown in Fig. 8. Fig. 8a showed the structure of the secondary alcohol hydroxyl group connected to C_4 at 0ps. At 17.6ps, the bond C_3-C_4 broke, as shown in Fig. 8b. At 41.06ps, the hydroxyl group attached to C_4 dehydrogenated to form carbonyl group, as shown in Fig. 8c. At 42.58ps, the bond C_4-C_5 broke, as shown in Fig. 8d. At 47.8ps, C_4 atom gained O atom to form C-O bonds, as shown in Fig. 8e. At 47.8ps, O atom deprived H to form formic acid molecule, as shown in Fig. 8f. Fig.9 shows the reaction formula of formic acid formation pathway 3. The key group carbonyl formed during the reaction that is marked with a dotted line. Statistics found that the number of formic acid molecules generated in this pathway was least. According to the structure of the cellulose molecular formula, the C atom connected to the secondary alcohol hydroxyl group contains two C-C bonds. According to the

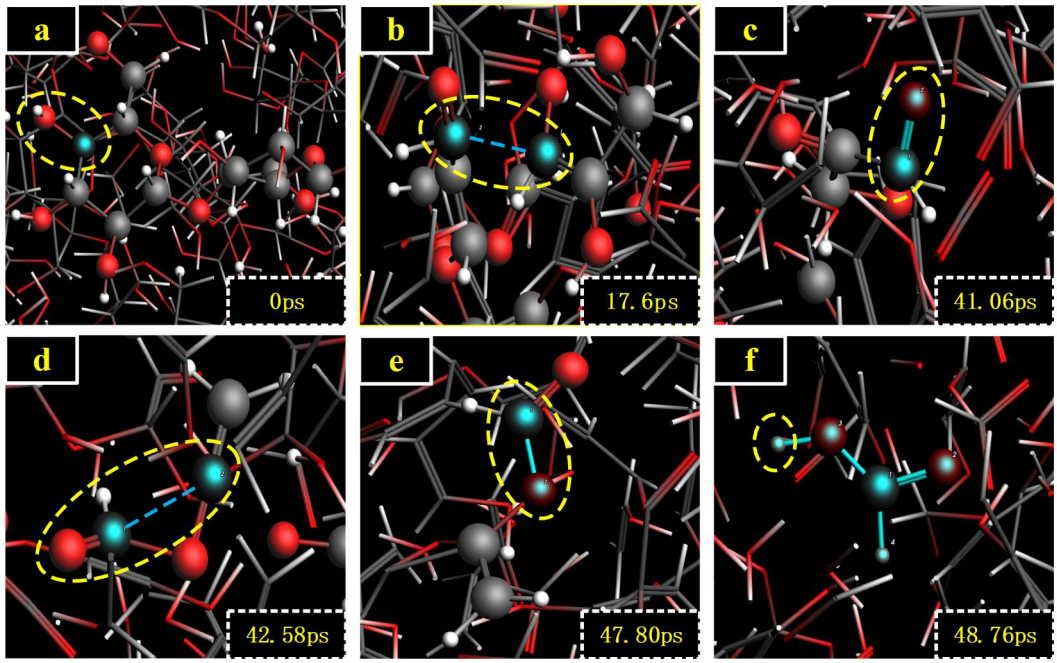

Fig.8 Microscopic formation process of formic acid molecules. The picture reveals the generation pathway 3 of formic acid molecule during the pyrolysis of cellulose molecules

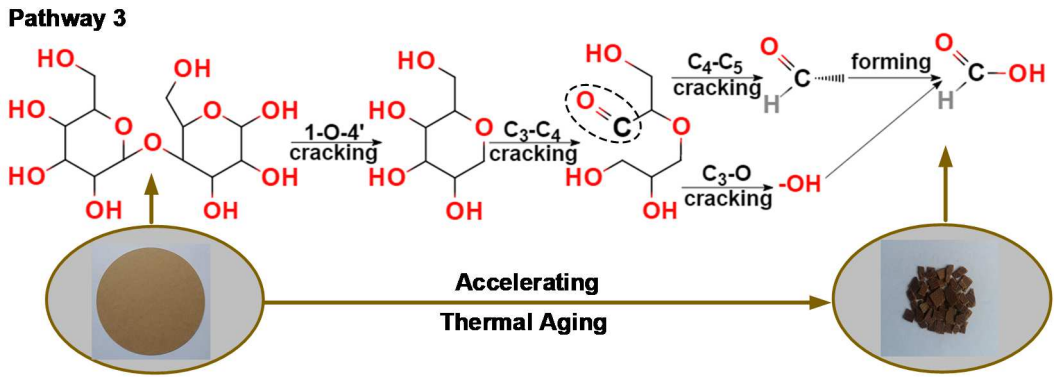

Fig. 9 Reaction formula of formic acid generation pathway 3. The pathway shows the breakage and formation of related chemical bonds

analysis of molecular electrostatic potential and the comparison of molecular chemical bond energy, it is known that this pathway is the most difficult to generate formic acid molecules.

Kinetic analysis of molecular model pyrolysis

The use of reactant consumption rate is to study pyrolysis kinetics that has been extensively studied (Chen et al. 2011; Ding et al. 2013). The molecular dynamics model assumes that the reactants have been completely pyrolyzed in these studies. To verify the reliability of the pyrolysis simulation, this paper studied the pyrolysis kinetics of cellulose molecule at 2200k-2600k.

$$\ln N_t - \ln N_0 = kt \tag{3}$$

$$\ln k = -\frac{E_a}{R}\frac{1}{T} + \ln A \quad (4)$$

Under the premise of ensuring accuracy, to quickly calculate the rate constant, the number of cellulose molecules was used instead of the concentration of the reactant. The linear fit between the number of molecules N_t and the simulation time t are shown in (3). The symbol N_0 represents the number of initial cellulose molecules, its value is 50. To calculate the rate constant k at a constant temperature T, the natural logarithm of the rate constant k and the reciprocal of the constant temperature were linearly fitted with $1/T$ firstly. As shown in formula (4), the activation energy E_a and the pre-exponential factor A were calculated through the Arrhenius expression. In formula (4), R is the molar gas constant, its value is about 8.3144J/(mol·K). Relevant data from the simulation study were used to calculate the rate constant k for many times through formula (3), then the Arrhenius formula (3) was used to linearly fit ln$k$ and $1/T$. As shown in Fig.10, the slope of the fit was -16.9849×10^3K·s^{-1}and the y-intercept was 31.5903s^{-1}. Finally, the calculated activation energy E_a was 135.3802kJ·mol^{-1} and the pre-exponential factor A was 3.8508×10^{13}s^{-1}. The calculated results are in line with the range of activation energy and pre-exponential factors summarized by many scholars on the kinetics of cellulose pyrolysis (Lin et al. 2009; Paajanen et al. 2017). The calculated results show that the pyrolysis results are all within the range of the above experimental results, verifies the reliability of the simulation research in this paper. Therefore, the simulation temperature is higher than the experimental temperature, which does not affect the simulation results. Meanwhile it shows the accuracy of using reactive molecular dynamics to study the aging of cellulosic insulating paper.

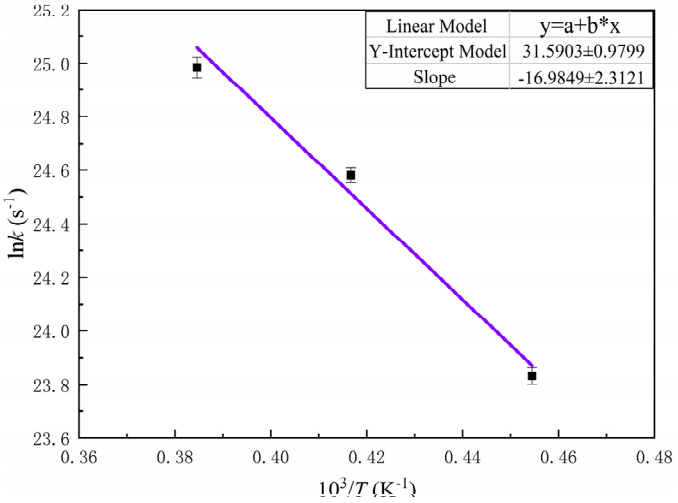

Fig.10 Fitted napierian logarithm of the rate constant k versus inverse temperature T obtained from the pyrolysis of DP-2 cellulose molecules at 2200K-2600K

Analysis of experimental result

It was detected by gas chromatography mass spectrometer that the aged cellulosic insulating paper generated formic acid molecules, which verified the accuracy of the simulation results. Meanwhile it shows the reliability of the BSTFA silanization derivatization method in detecting formic acid molecules. The silylation reaction between the silylation reagent BSTFA and formic acid is that the methylsilyl group in BSTFA replaces the carboxyl hydrogen in formic acid, which generates formic acid TMS derivative (Bugelytė et al. 2019). The reaction formula is shown in Fig. 11. Fig.12 shows the detection results of the formic acid derivative by gas chromatography mass spectrometer. Fig. 12 a denotes the mass spectrum of the target component. Fig. 12b denotes the mass spectrum in the National Institute of Standards and Technology database. The obtained mass spectrum is compared with the database, it further confirms that the target component is a formic acid derivative. Fig. 12c shows the chromatogram of formic acid derivative, which shows the retention time of the chromatographic peak of formic acid derivative.

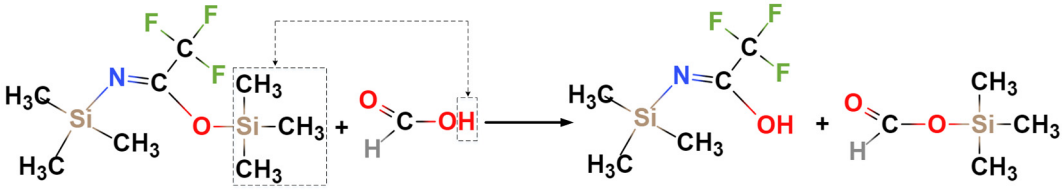

Fig. 11 Reaction formula of BSTFA and formic acid generating the formic acid TMS derivatives

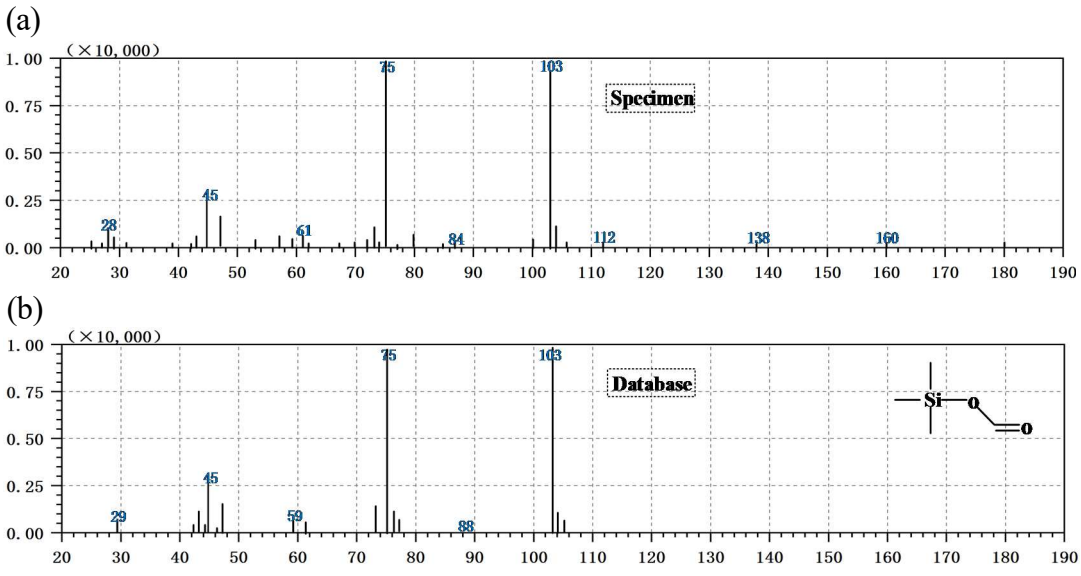

(c)

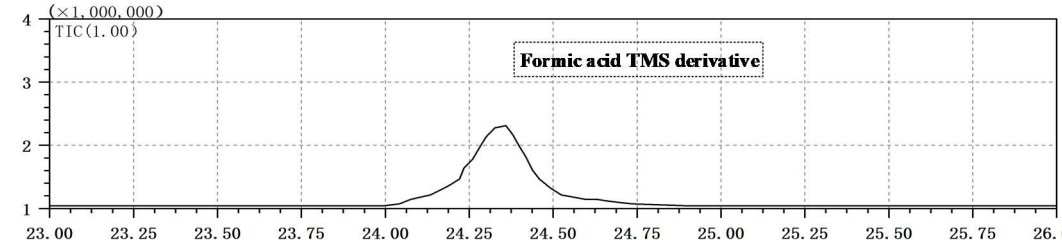

Fig. 12 Results of detection of formic acid derivatives by gas chromatography mass spectrometer

Conclusion

This paper used ReaxFF-MD simulation and accelerated aging experiments to study the pyrolysis of insulating paper. ReaxFF-MD was used to observe the formation and breaking of chemical bonds at the atomic level, which analyzed the generation pathways of formic acid at different temperatures. The kinetic model was used to describe the pyrolysis process of cellulosic insulating paper. The calculated activation energy E_a is 135.3802kJ·mol^{-1} and the pre-exponential factor A is 3.8508×10^{13}s^{-1}. The results are in line with the existing experimental data and Arrhenius's law, which verifies the accuracy of ReaxFF-MD simulation at the atomic level to study the pyrolysis of cellulosic insulating paper.

This paper analyzed the pyrolysis of cellulose molecules to generate formic acid molecules at 1600K-2600K. It showed that formic acid molecules were the main product of cellulose pyrolysis. As the pyrolysis temperature rised, the rate of rise in the number of formic acid molecules increased. When the pyrolysis temperature rised, the peak time of the number of formic acid molecules would be advanced. The number of formic acid molecules decreased slightly after its number reached the maximum. The number of formic acid molecules would fluctuate during the pyrolysis process. Through the analysis of the generation pathways of formic acid molecules, it was found that the generation of formic acid can be divided into three pathways. The first pathway is that the ether group oxygen atom O_5(O'_5) and C_1(C'_1) form carbonyl group to generate formic acid molecule. In this pathway, formic acid is directly generated through molecular bond breaking. The second pathway is that formic acid molecule is generated after the primary alcohol hydroxyl group dehydrogenates to form carbonyl group. In this pathway, formic acid is generated through secondary reaction. The reaction generates formaldehyde molecule that dehydrogenates and grabs hydroxyl group to generate formic acid molecule. The third pathway is that formic acid molecule is generated after the secondary alcohol

hydroxyl group dehydrogenates to form carbonyl group. After the hydroxyl group dehydrogenates to form a carbonyl group, the C-C bond is broken, and formic acid molecule is generated after the capture of hydroxyl group reaction occurs. According to statistics, it is found that the generation of formic acid molecules mainly comes from the first pathway. When the pyrolysis temperature and pyrolysis time increase, the generation of formic acid molecules appears in the latter two pathways. The latter two pathways generate a smaller number of formic acid molecules.

Though analysis of simulation results, it was found that formic acid appeared in the early stage of pyrolysis and stably existed in the later stage of pyrolysis. In the later stage of aging, the formic acid generated by the pyrolysis of cellulosic insulating paper continued to increase, it would diffuse into the insulating oil. This paper designed oil-paper insulation accelerated thermal aging experiments, the samples were silanized with BSTFA reagent. Finally, it was detected by gas chromatography mass spectrometer that a large amount of formic acid was generated due to the aging of cellulosic insulating paper. It further verified the feasibility of formic acid as an assessment of the aging state of cellulosic insulating paper. This also showed the reliability of BSTFA silanization derivatization method in detecting formic acid in oil paper insulation.

Declaration of Competing Interest

The authors declare that they have no known competing financial interests or personal relationships that could have appeared to influ-ence the work reported in this paper.

Acknowledge

This work was supported in part by the National Natural Science Foundation of China under Grant 51907034, in part by the Guangxi Science and Technology Base and Talent Project under Grant 2020AC19010, and in part by the Natural Science Foundation of Guangxi under Grant 2018JJB160056.

References

Azis N, Liu Q, Wang ZD (2014) Ageing assessment of transformer paper insulation through post mortem analysis. IEEE Trans Dielectr Electr Insul 21(2): 845–853

Bugelytė B, llonina K, Poškus V, et al (2019) Gas chromatographic determination of some carboxylic acids: comparison between solution and headspace analysis. Chemija 30(4):227-233

Chenoweth K, Van Duin ACT, Goddard WA (2008) ReaxFF reactive force field for molecular dynamics simulations of hydrocarbon oxidation. J Phys Chem A 112:1040–1053

Chen WH, Kuo PC (2011) Isothermal torrefaction kinetics of hemicellulose, cellulose, lignin and xylan using thermogravimetric analysis. Energy 36(11):6451–6460

Cui Y, Wu G, Wang X, et al (2013) The influence of organic acid on thermal aging of power transformer oil-paper insulation. In 2013 Annual Report Conference on Electrical Insulation and Dielectric Phenomena. IEEE, pp 116–119

Ding J, Zhang L, Zhang Y et al (2013) A reactive molecular dynamics study of n-heptane pyrolysis at high temperature. J Phys Chem A 117:3266–3278

Du D, Tang C, Yang L, et al (2020) Molecular dynamics simulation on the distribution and diffusion of different sulfides in oil-paper insulation systems. J Mol Liq 314: 113678

English NJ, Waldron CJ (2015) Perspectives on external electric fields in molecular simulation: progress, prospects and challenges. Phys Chem Chem Phys 17(19): 12407-12440

Ese MG, Liland KB, Lesaint C, et al (2014) Esterification of low molecular weight acids in cellulose. IEEE Trans Dielectr Electr Insul 21(2):662-665

Gao S, Yang L, Ke T (2020) Failure mechanism of transformer oil-immersed cellulosic insulation induced by sulfur corrosion. Cellulose https://doi.org/10.1007/s10570-020-03271-x

Gao Y, Wang X, Yang H, et al (2012) Characterization of products from hydrothermal treatments of cellulose. Energy 42(1):457–465

Gao Z, Li N, Chen M, et al (2019) Comparative study on the pyrolysis of cellulose and its model compounds. Fuel Process Technol 193:131–140

542 Ingebrigtsen S, Dahlund M, Hansen W, et al (2004) Solubility of carboxylic acids
543 in paper (Kraft)-oil insulation systems. In: The 17th Annual Meeting of the
544 IEEE Lasers and Electro-Optics Society (LEOS). IEEE, pp 253-257
545 Kouassi KD, Fofana I, Cissé L, et al (2018) Impact of Low Molecular Weight Acids
546 on Oil Impregnated Paper Insulation Degradation. Energies 11(6):1465
547 Lelekakis N, Wijaya J, Martin D, et al (2014) The effect of acid accumulation in
548 power-transformer oil on the aging rate of paper insulation. IEEE Electr Insul
549 Mag 30(33):19–26
550 Li X, Tang C, Wang J, et al (2019) Analysis and mechanism of adsorption of
551 naphthenic mineral oil, water, formic acid, carbon dioxide, and methane on
552 meta-aramid insulation paper. J Mater Sci 54(11): 8556-8570
553 Lin Y, Cho J, Tompsett GA et al (2009) Kinetics and mechanism of cellulose
554 pyrolysis. J Phys Chem C 113:20097–20107
555 Lu T, Chen F (2012) Quantitative analysis of molecular surface based on improved
556 marching tetrahedra algorithm. J Mol Graphics Modell 38:314–323
557 Lundgaard LE, Hansen W, Ingebrigtsen S, et al (2005) Aging of kraft paper by acid
558 catalyed hydrolysis. In: 2005 IEEE International Conference on Dielectric
559 Liguids (ICDL). IEEE, pp381–384
560 Lundgaard LE, Hansen W, Ingebrigtsen S (2008) Ageing of mineral oil
561 impregnated cellulose by acid catalysis. IEEE Trans Dielectr Electr Insul
562 15(2): 540–546
563 Lundgaard LE, Hansen W, Linhjell D, et al (2004) Aging of oil-impregnated paper
564 in power transformers. IEEE Trans Power Delivery 19(1):230–239
565 Mazeau K, Heux L (2003) Molecular dynamics simulations of bulk native
566 crystalline and amorphous structures of cellulose. J Phys Chem B 107:2394–
567 2403
568 Mo W, Huang Q, Song H, et al (2016) Influence of Acids on the Electrical Lifetime
569 of Vegetable Oil Impregnated Paper Insulation. In: 2016 IEEE International
570 Conference on High Voltage Engineering and Application (ICHVE). IEEE, pp
571 1-4
572 Ojha SK, Purkait P, Chakravorti S (2017) Evaluating the effects of lower molecular
573 weight acids in oil-paper insulated transformer. In 2017 3rd International
574 Conference on Condition Assessment Techniques in Electrical Systems
575 (CATCON). IEEE, pp 138–143

576 Paajanen A, Vaari J (2017) High-temperature decomposition of the cellulose
577 molecule: a stochastic molecular dynamics study. Cellulose 24(7): 2713–2725
578 Shi L, Zhao T, Shen G et al (2016) Molecular dynamics simulation on generation
579 mechanism of water molecules during pyrolysis of insulating paper. In: 2016
580 IEEE international conference on high voltage engineering and application
581 (ICHVE). IEEE, pp 1–4
582 Sørensen MR, Voter AF (2000) Temperature-accelerated dynamics for simulation
583 of infrequent events. J Chem Phys 112:9599–9606
584 Standard BOI (2006) IEC-60599-2007 Edition 2.1 Mineral oil impregnated
585 electrical equipment in services—guide to the interpretation of dissolved and
586 free gases analysis
587 Šťávová J, Beránek J, Nelson EP, et al (2011) Limits of detection for the
588 determination of mono-and dicarboxylic acids using gas and liquid
589 chromatographic methods coupled with mass spectrometry. J Chromatogr B
590 879(17-18): 1429-1438
591 Tang C, Zhang S, Li X, et al (2015) Experimental analyses and molecular
592 simulation of the thermal aging of transformer insulation paper. IEEE Trans
593 Dielectr Electr Insul 22(6): 3608-3616
594 Tang J, Song Y, Zhao F, et al (2019) Compressible cellulose nanofibril (CNF) based
595 aerogels produced via a bio-inspired strategy for heavy metal ion and dye
596 removal. Carbohydr Polym 208: 404–412
597 Tang Q, Yan W, Wang N, et al (2017) Study on oil-paper insulation aging based on
598 multi-characteristic parameters. In: 2017 Chinese Automation Congress
599 (CAC). IEEE, pp 5197–5201
600 Tojo G, Fernández M (2007) Oxidation of primary alcohols to carboxylic acids. A
601 Guide to Current Common Practice, pp 105-109
602 Urquiza D, Garcia B, Burgos JC (2015) Statistical study on the reference values of
603 furanic compounds in power transformers. IEEE Electr Insul Mag 4(31):15–
604 23
605 Vahidi F, Tenbohlen S, Rapp K, et al (2017) Electrical conductivity of oil and oil-
606 impregnated pressboard dependent on aging byproducts. In: 2017
607 International Symposium on Electrical Insulating Materials (ISEIM). IEEE,
608 pp 712-715

609 Van Duin ACT, Dasgupta S, Lorant F et al (2001) ReaxFF: a reactive force field
610 for hydrocarbons. J Phys Chem A 105:9396–9409
611 Wada J, Ueta G, Okabe S, et al (2014) Method to evaluate the degradation condition
612 of transformer insulating oil-experimental study on the hydrophilic and
613 dissociative properties of degradation products. IEEE Trans Dielectr Electr
614 Insul 21(2): 873-881
615 Wang D, Zhu Z, Zhang L, et al (2019) Influence of metal transformer materials on
616 oil-paper insulation after thermal aging. IEEE Trans Dielectr Electr Insul
617 26(2):554–560
618 Wang S, Dai G, Ru B et al (2017) Influence of torrefaction on the characteristics
619 and pyrolysis behavior of cellulose. Energy 120:864–871
620 Wang Z, Yi X, Huang J, et al (2012) Fault gas generation in natural-ester fluid under
621 localized thermal faults. IEEE Electr Insul Mag 28(6):45-56
622 Zhang Y, Li Y, Zheng H, et al (2020) Microscopic reaction mechanism of the
623 production of methanol during the thermal aging of cellulosic insulating paper.
624 Cellulose 27(5): 2455-2467
625 Zheng H, Shi K, Yang T, et al (2020) Investigation on the equilibrium distribution
626 of methanol in transformer oil-immersed cellulosic insulation. Cellulose
627 https://doi.org/10.1007/s10570-020-03608-6
628 Zhang E, Zheng H, Zhang C, et al (2021) Aging state assessment of transformers
629 cellulosic paper insulation using multivariate chemical indicators. Cellulose
630 https://doi.org/10.1007/s10570-021-03683-3
631 Zheng M, Wang Z, Li X, et al (2016) Initial reaction mechanisms of cellulose
632 pyrolysis revealed by ReaxFF molecular dynamics. Fuel 177:130–141

Figures

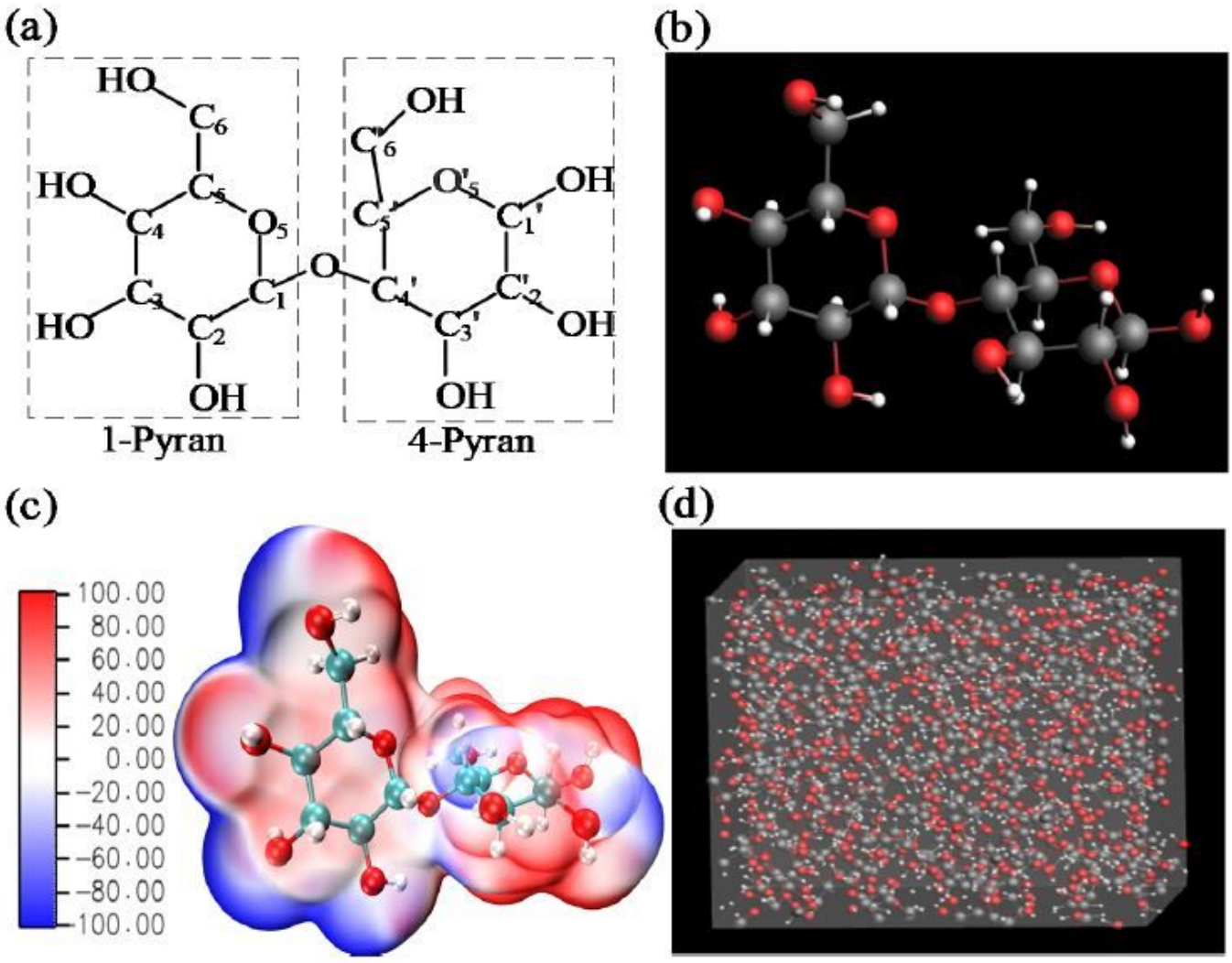

Figure 1

a The main atoms of DP-2 cellulose molecule. b Molecular model of DP-2 cellulose molecule. c Electrostatic potential distribution on the surface of DP-2 cellulose molecule. d Amorphous unit cell optimized model.

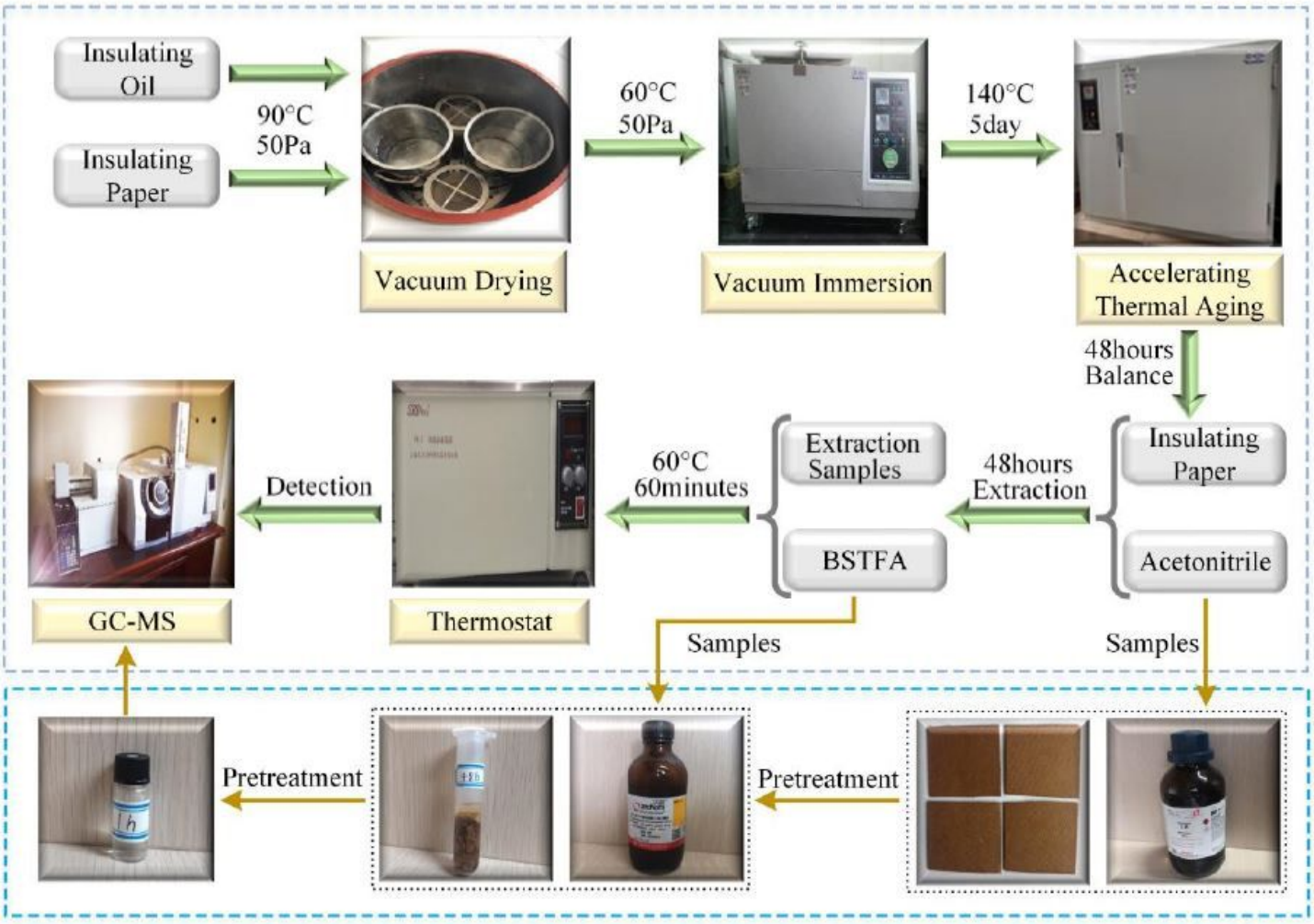

Figure 2

Oil-paper insulation thermal aging experiment and silanization detection for formic acid

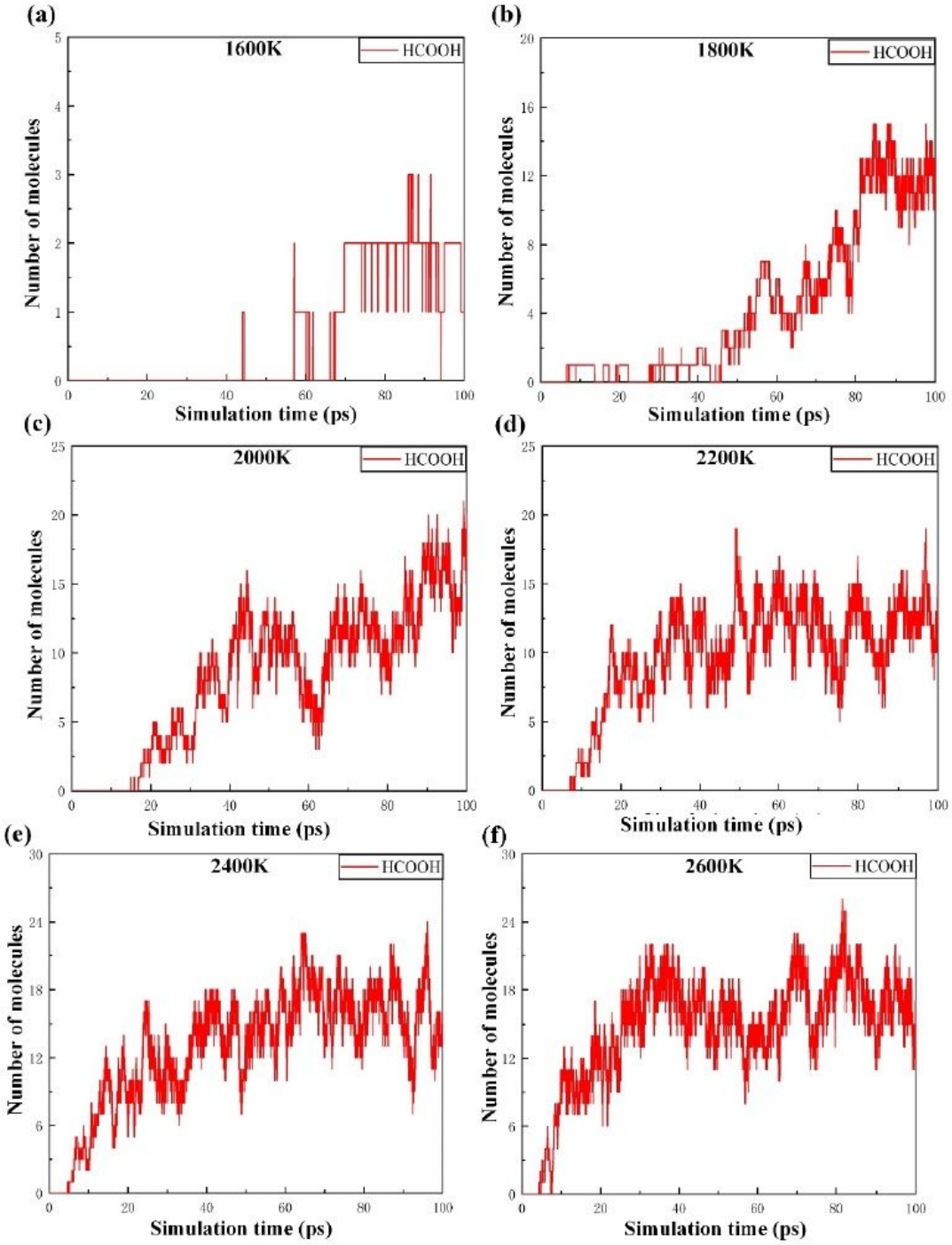

Figure 3

Change curves of the number of formic acid molecules with pyrolysis time at 1600K- 2600K

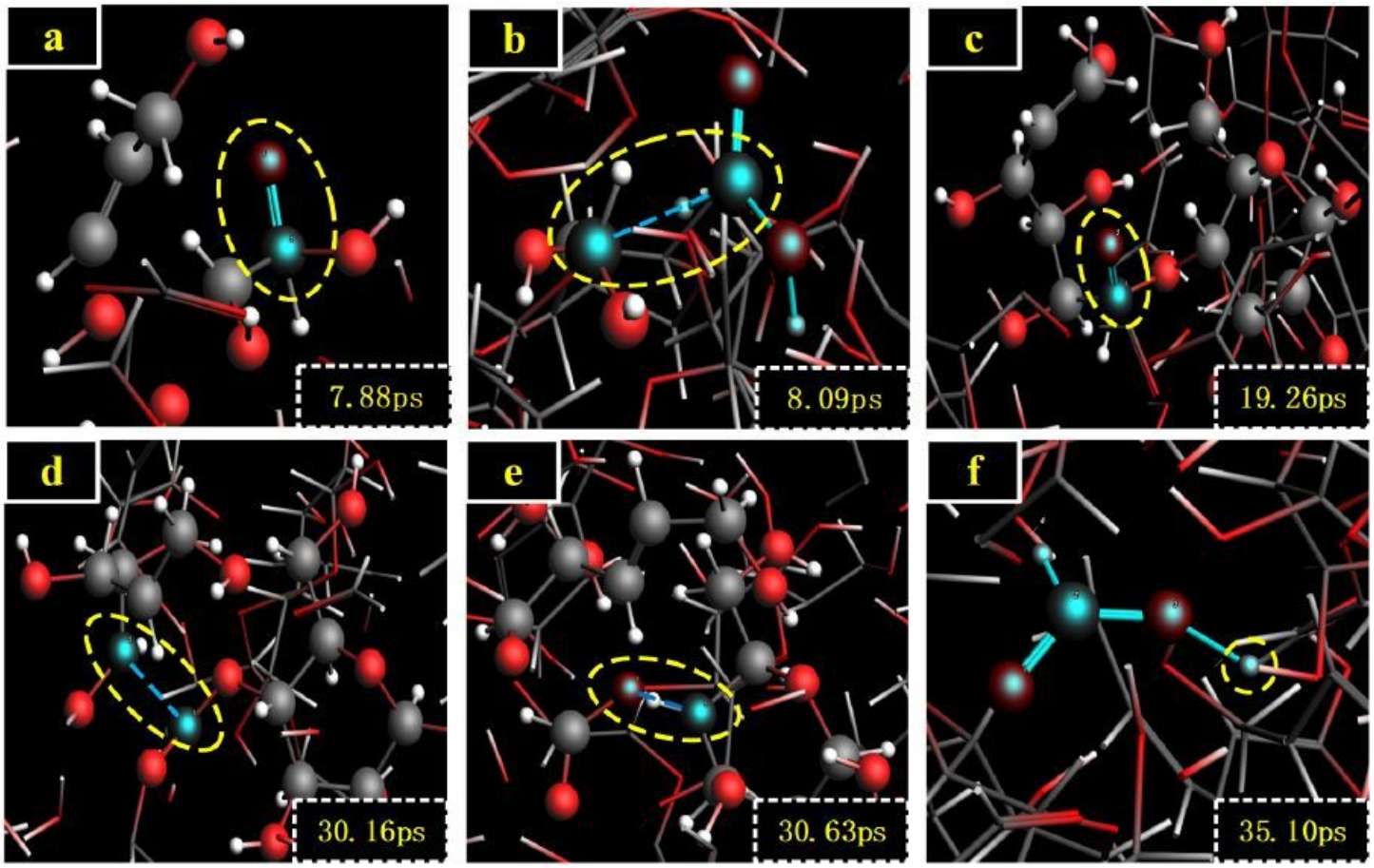

Figure 4

Microscopic formation process of formic acid molecules. The picture reveals the generation pathway 1 of formic acid molecule during the pyrolysis of cellulose molecules

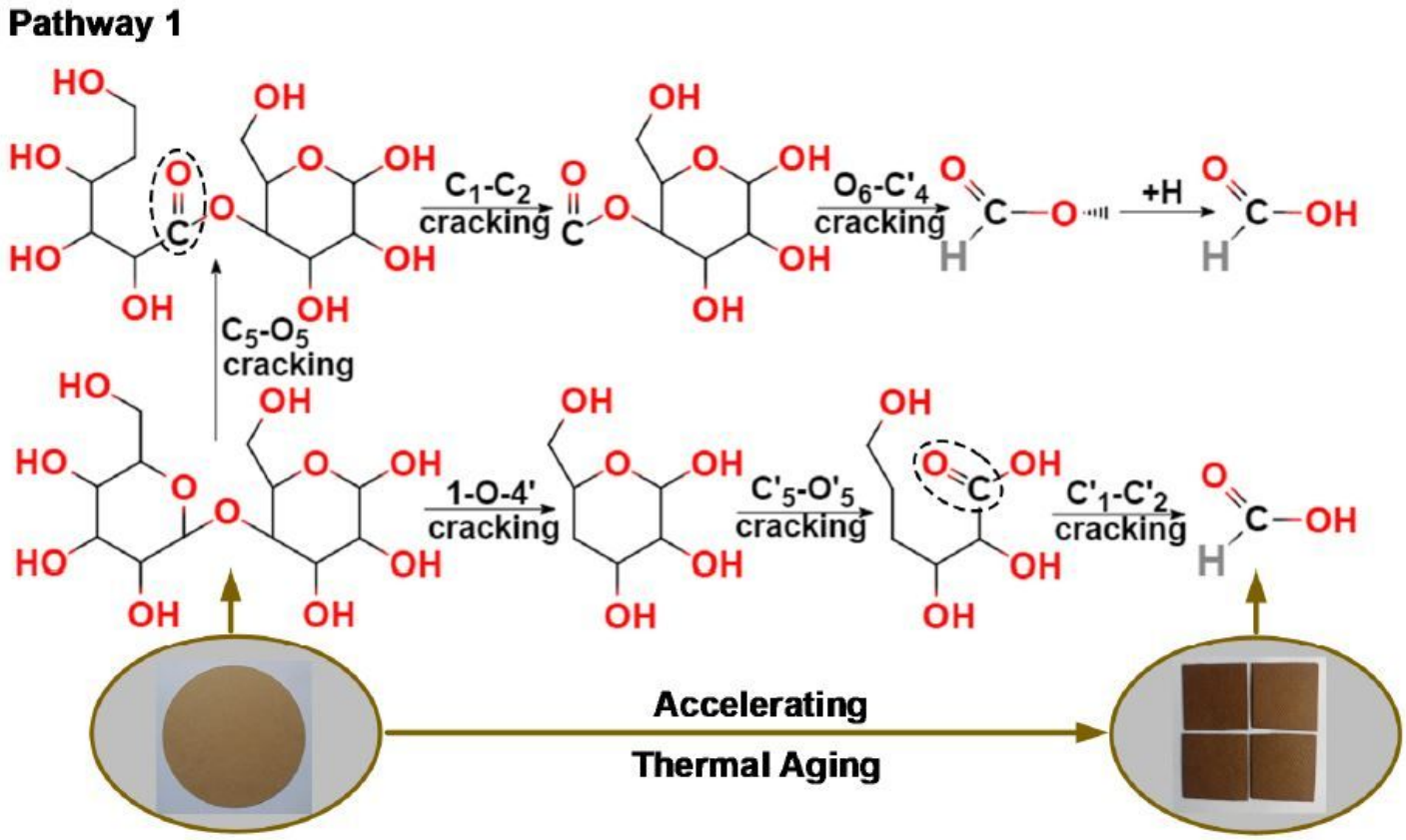

Figure 5

Reaction formula of formic acid generation pathway 1. The pathway shows the breakage and formation of related chemical bonds

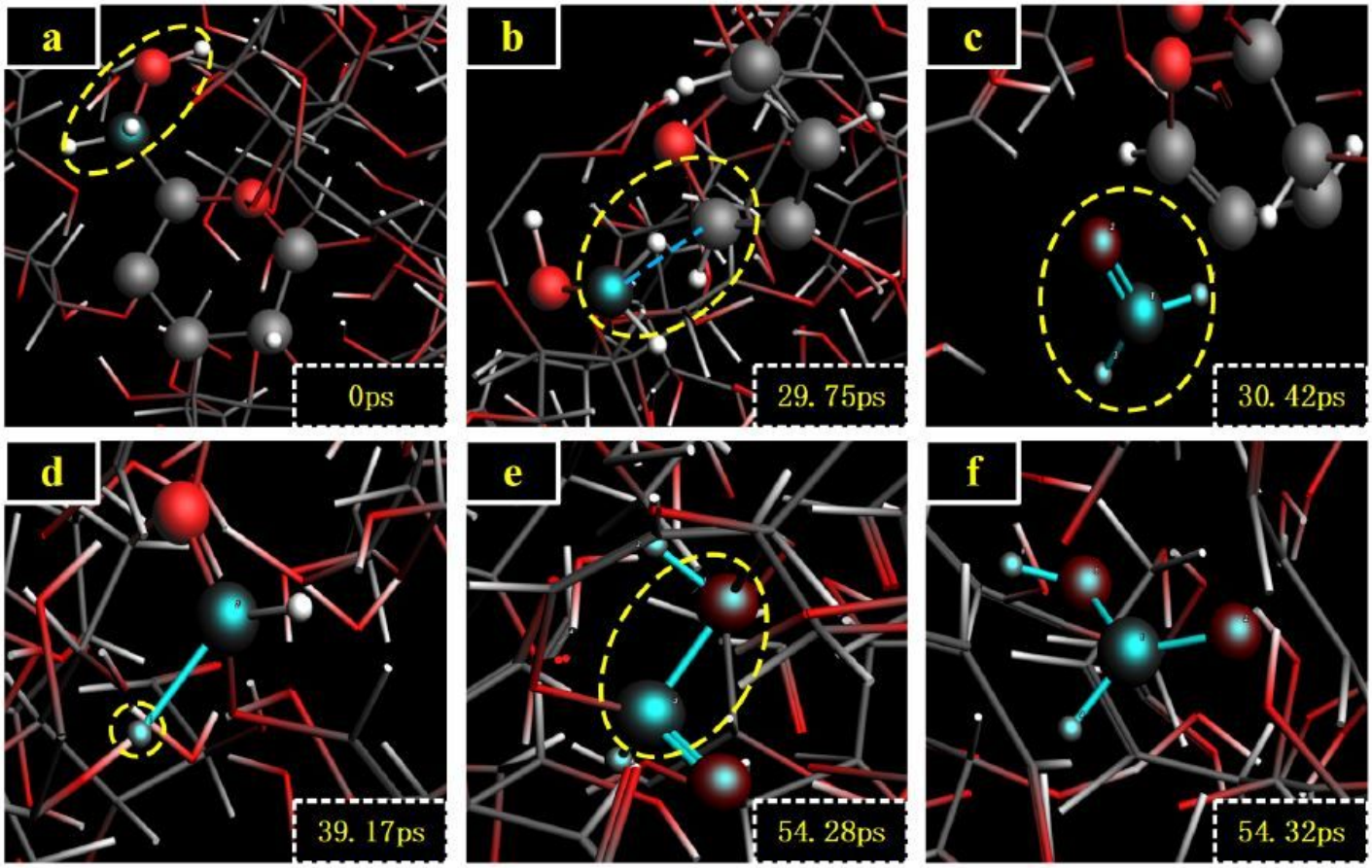

Figure 6

Microscopic formation process of formic acid molecules. The picture reveals the generation pathway 2 of formic acid molecule during the pyrolysis of cellulose molecules

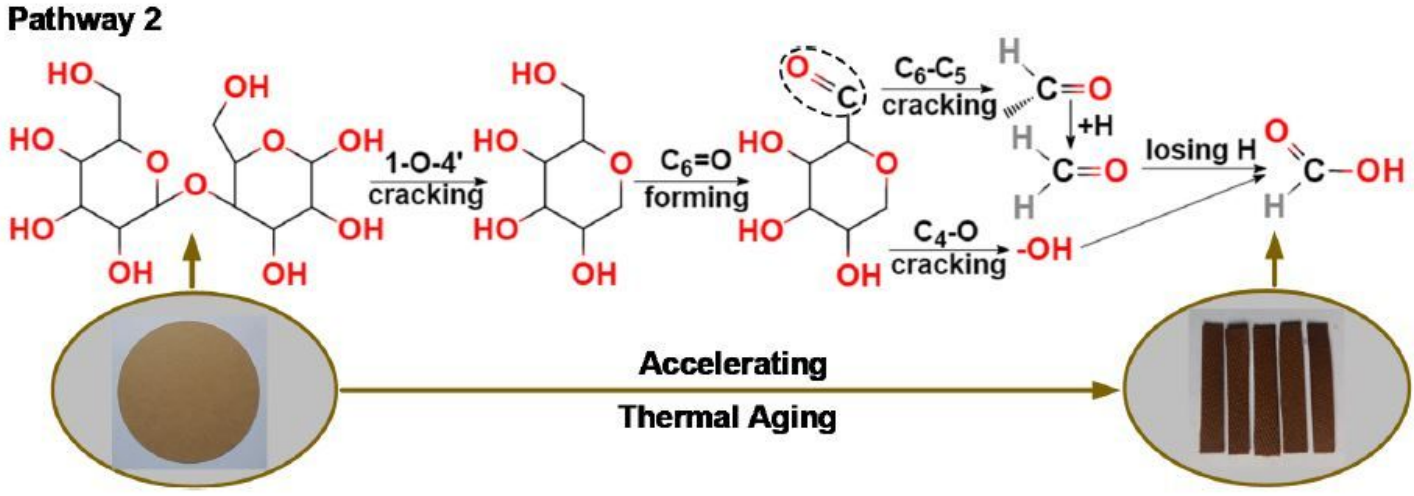

Figure 7

Reaction formula of formic acid generation pathway 2. The pathway shows the breakage and formation of related chemical bonds

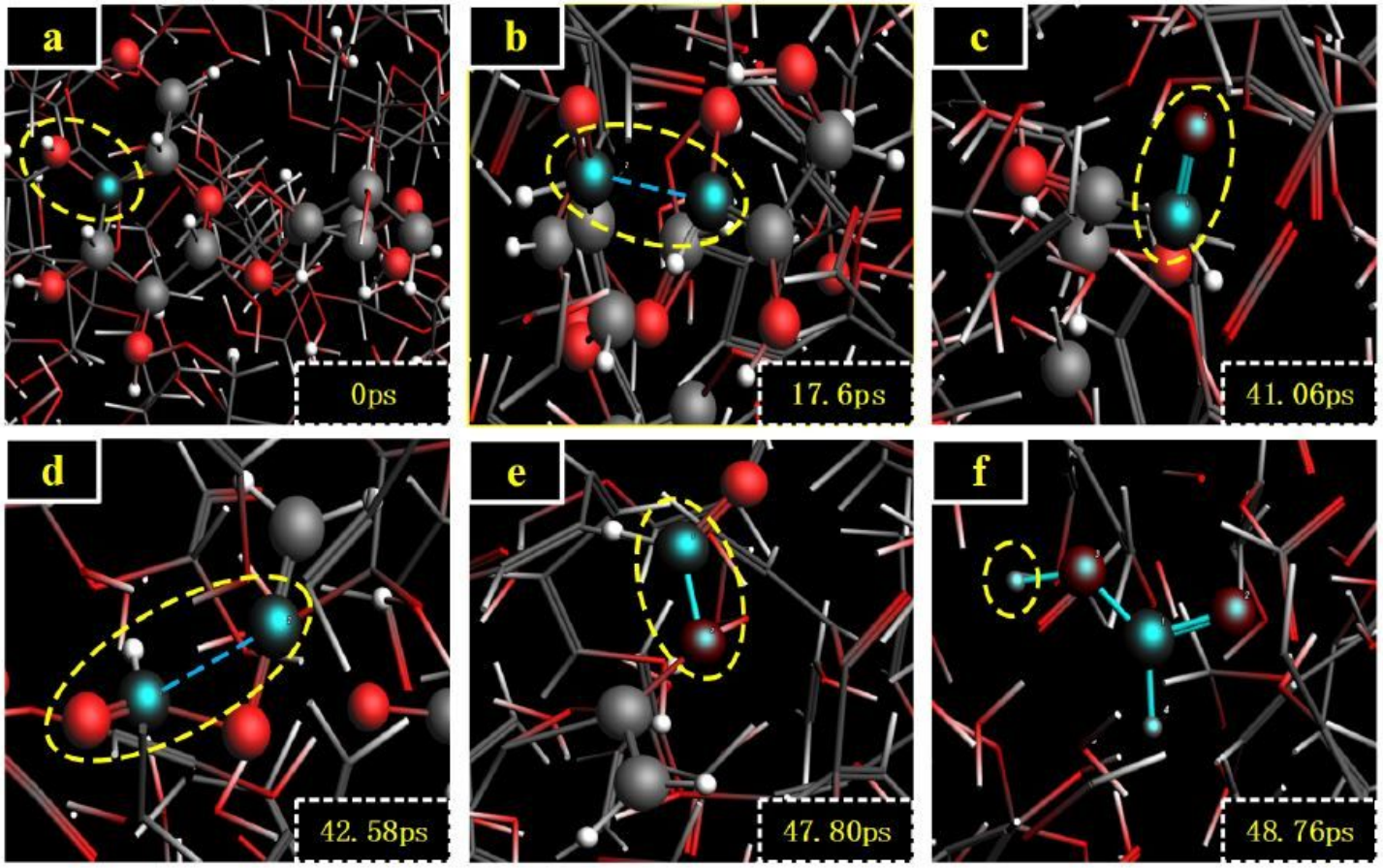

Figure 8

Microscopic formation process of formic acid molecules. The picture reveals the generation pathway 3 of formic acid molecule during the pyrolysis of cellulose molecules

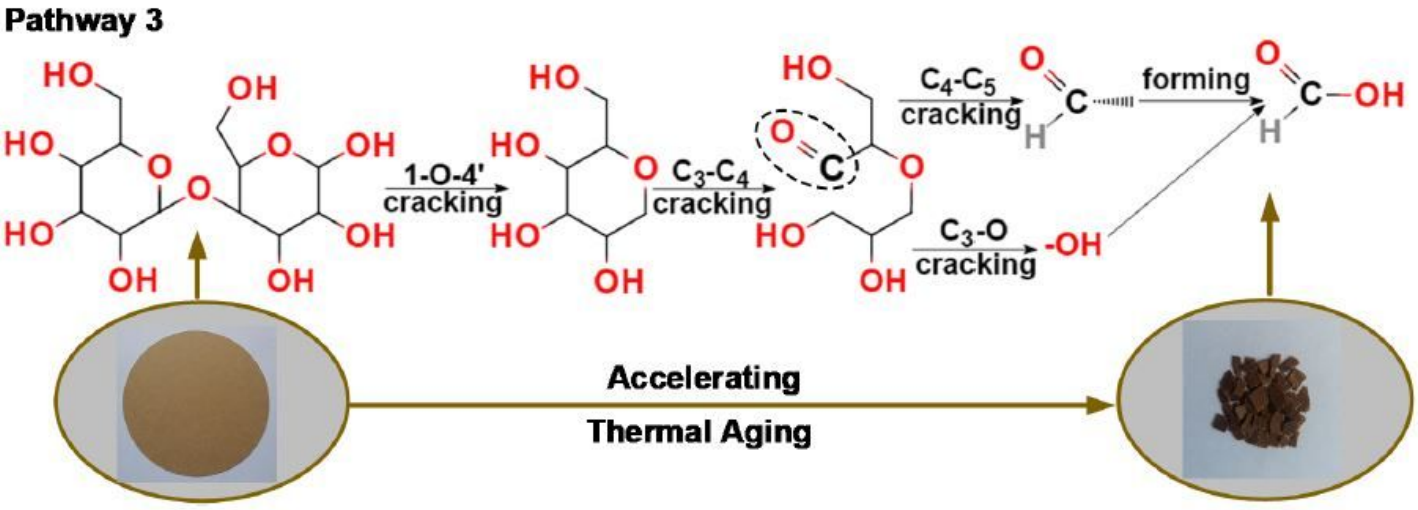

Figure 9

Reaction formula of formic acid generation pathway 3. The pathway shows the breakage and formation of related chemical bonds

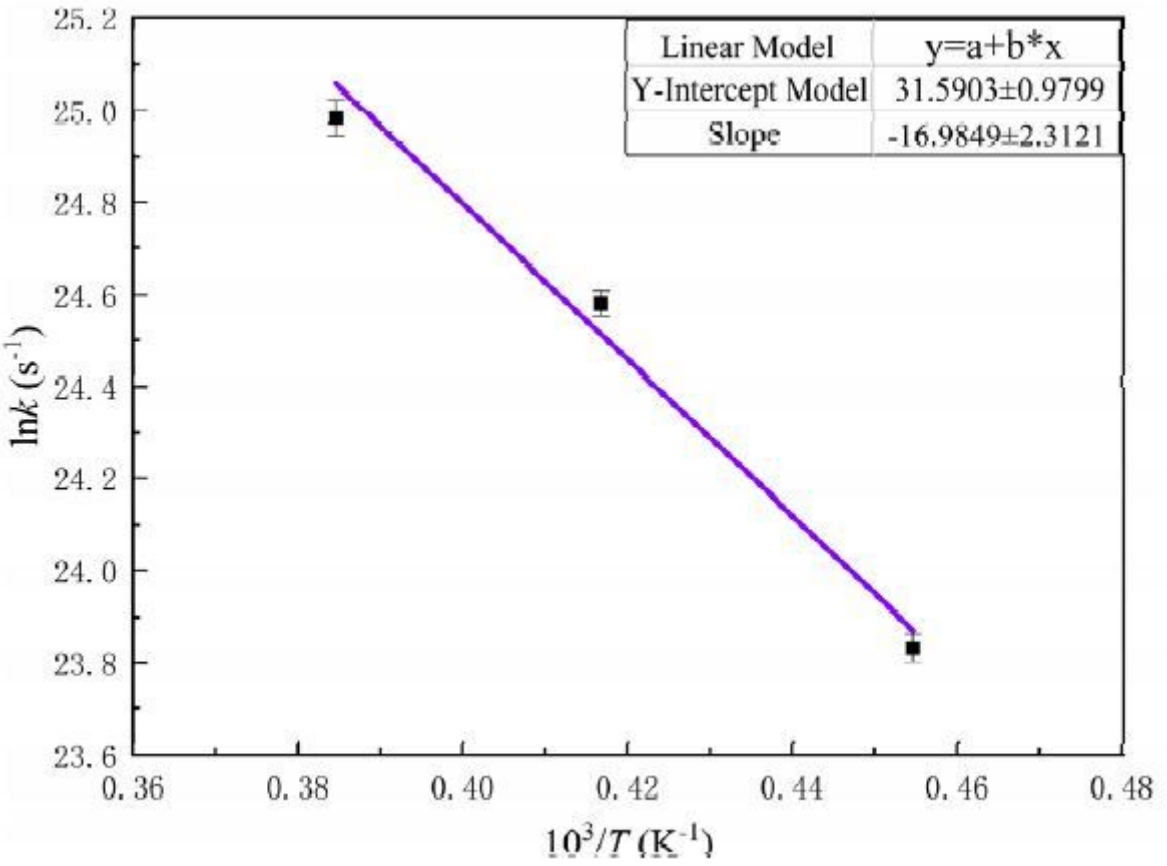

Figure 10

Fitted napierian logarithm of the rate constant k versus inverse temperature T obtained from the pyrolysis of DP-2 cellulose molecules at 2200K-2600K

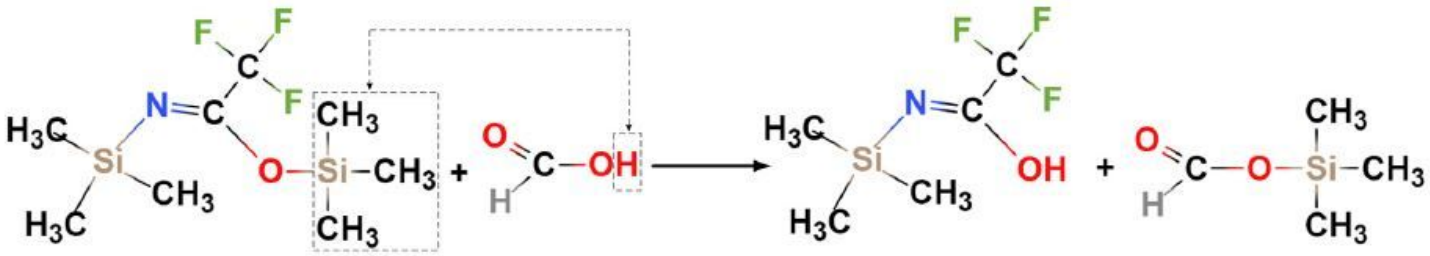

Figure 11

Reaction formula of BSTFA and formic acid generating the formic acid TMS derivatives

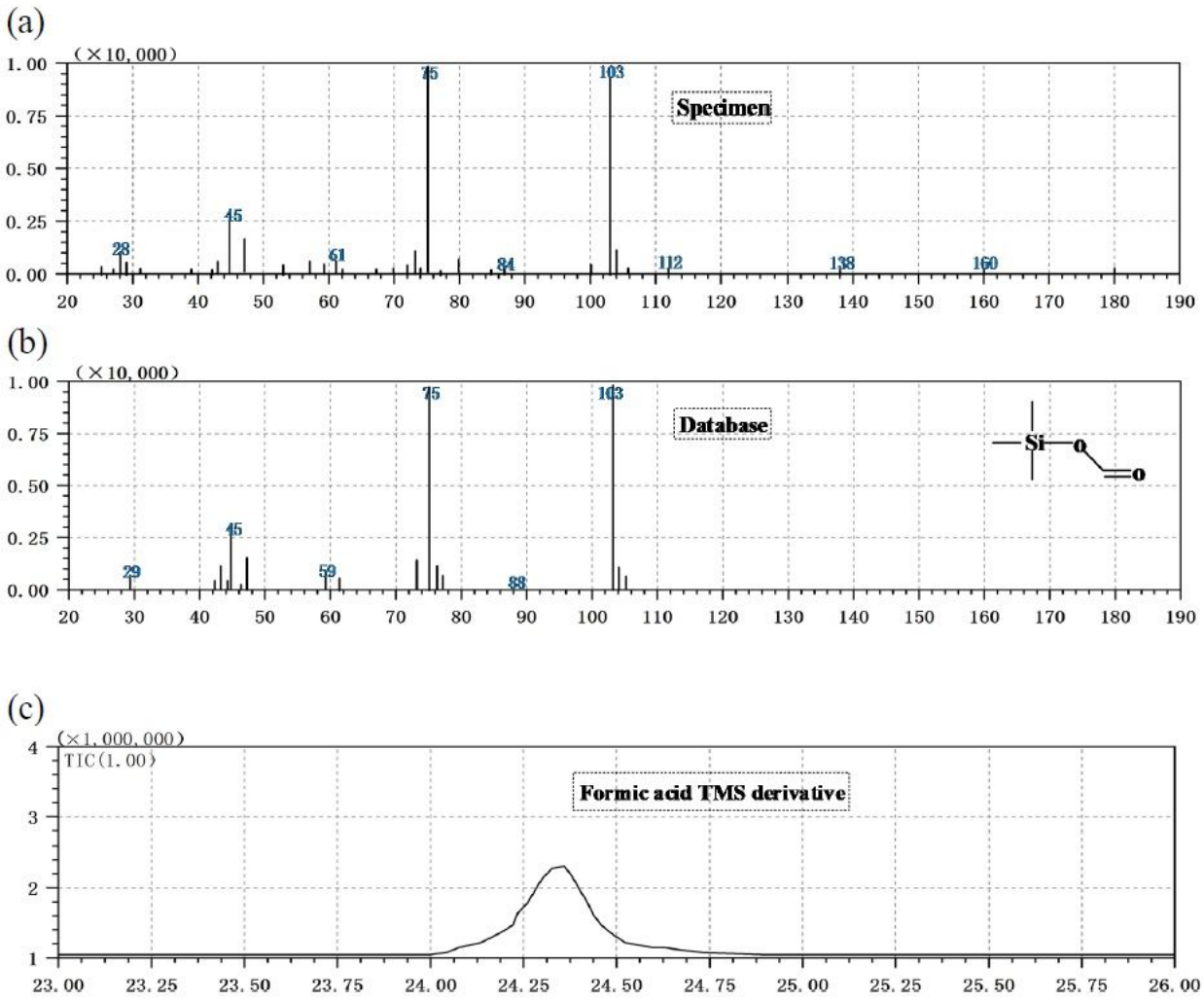

Figure 12

Results of detection of formic acid derivatives by gas chromatography mass spectrometer

Supplementary Files

This is a list of supplementary files associated with this preprint. Click to download.

- GraphicalAbstract.docx